Isotope shifts and hyperfine structure in the 555.8-nm $^1S_0 \rightarrow {}^3P_1$ line of Yb

Kanhaiya Pandey, Alok K. Singh, P. V. Kiran Kumar,* M. V. Suryanarayana,* and Vasant Natarajan†
Department of Physics, Indian Institute of Science, Bangalore 560 012, India

(Received 28 May 2009; revised manuscript received 8 July 2009; published 31 August 2009)

We apply our technique of using a Rb-stabilized ring-cavity resonator to measure the frequencies of various spectral components in the 555.8-nm $^1S_0 \rightarrow {}^3P_1$ line of Yb. We determine the isotope shifts with 60 kHz precision, which is an order-of-magnitude improvement over the best previous measurement on this line. There are two overlapping transitions, ^{171}Yb$(1/2 \rightarrow 3/2)$ and ^{173}Yb$(5/2 \rightarrow 3/2)$, which we resolve by applying a magnetic field. We thus obtain the hyperfine constants in the $^3P_1$ state of the odd isotopes with a significantly improved precision. Knowledge of isotope shifts and hyperfine structure should prove useful for high-precision calculations in Yb necessary to interpret ongoing experiments testing parity and time-reversal symmetry violation in the laws of physics.

DOI: 10.1103/PhysRevA.80.022518 PACS number(s): 31.30.Gs, 32.10.Fn, 32.30.Jc

I. INTRODUCTION

Precise measurements of isotope shifts and hyperfine structure in atomic lines provide valuable information about the structure of the nucleus. Isotope shifts provide information about the change in charge distribution between isotopes, and hyperfine structure gives information about the electric and magnetic moments of the nucleus. In addition, comparison between calculated and measured values of hyperfine constants acts as a stringent check on atomic wave functions used in theoretical calculations. This is particularly important in heavy atoms such as Yb because they are proposed to be used in studies of atomic parity violation [1] and the search for a permanent electric dipole moment [2]. In these experiments, the experimental results can be related to fundamental theories only if the atomic wave functions are known with sufficient accuracy [3].

We have recently developed a technique for measuring the absolute frequencies of optical transitions with uncertainty below 60 kHz [4–7]. The technique uses an evacuated ring-cavity resonator whose length is calibrated against a reference laser locked to the D_2 line of ^{87}Rb. The frequency of the reference transition is known with 6 kHz precision, allowing similar high precision in the measurement of the unknown transition. We had earlier applied this technique to the measurement of isotope shifts and hyperfine structure in the 399-nm $^1S_0 \leftrightarrow {}^1P_1$ line in Yb [5,8]. In this work, we measure the transition frequencies of spectral components in the other important line in Yb, namely, the 555.8-nm $^1S_0 \leftrightarrow {}^3P_1$ intercombination line. Although we measure the absolute frequencies of various transitions, temperature-dependent dispersion inside the cavity allows only the difference frequencies to be determined with a high precision. However, our accuracy is still an order of magnitude better than a previous measurement on this line [9], which used a Fabry-Perot cavity to reach an accuracy of 500 kHz. There are two overlapping transitions for the odd isotopes, and we use a magnetic field to separate the sublevels. This allows us to determine the hyperfine constants in the $^3P_1$ state of the odd isotopes, again with a significantly improved precision.

II. EXPERIMENTAL DETAILS

Our frequency-measurement technique uses the fact that the frequency of the 780-nm D_2 line in ^{87}Rb ($5S_{1/2} \leftrightarrow 5P_{3/2}$ transition) is known with an accuracy of 6 kHz [10]. A diode laser locked to this line is used as a frequency reference. A second laser is in turn locked to the unknown transition. The two lasers are coupled into an evacuated ring-cavity resonator. An acousto-optic modulator (AOM) placed in the path of one of the two lasers is used to produce a small frequency offset (on the order of 100 MHz), so that the cavity is in simultaneous resonance with both laser frequencies. Thus, the ratio of the unknown frequency to the reference frequency is just a ratio of two integers (i.e., the respective cavity mode numbers) combined with the AOM offset. The procedure to determine the unique mode-number combination for the two lasers has been described extensively in our earlier work [6]. We have used this technique to measure frequencies of transitions in the range of 670–895 nm (i.e., ± 100 nm away from the reference wavelength) with an accuracy of 60 kHz. The accuracy in the previous measurements was primarily limited by the linewidth of the transition, which was on the order of 10 MHz. One of the primary advantages of the technique is that we can check for systematic errors by locking the reference laser to different hyperfine transitions, varying in frequency by a few GHz.

The schematic of the experiment is shown in Fig. 1. The reference laser is a homebuilt diode laser [11] with a linewidth of about 1 MHz. It is locked to the D_2 line of ^{87}Rb using saturated-absorption spectroscopy in a vapor cell. The laser used to access the Yb line is a frequency-doubled fiber laser (Koheras, The Netherlands). The fiber laser output is at 1111.6 nm with a linewidth of 50 kHz. The doubled output at 555.8 nm is passed through AOM1 for Yb spectroscopy and locking to a particular transition. The cavity length of the resonator is locked to this laser. The reference laser is frequency shifted using AOM2 before entering the cavity, and the fixed cavity length is used to lock the frequency of

*Permanent address: National Centre for Compositional Characterisation of Materials, ECIL (PO), Hyderabad 500 062, India.
†vasant@physics.iisc.ernet.in; www.physics.iisc.ernet.in/~vasant

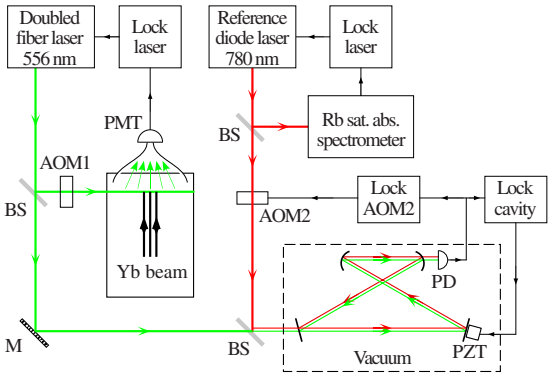

FIG. 1. (Color online) Schematic of the experiment.

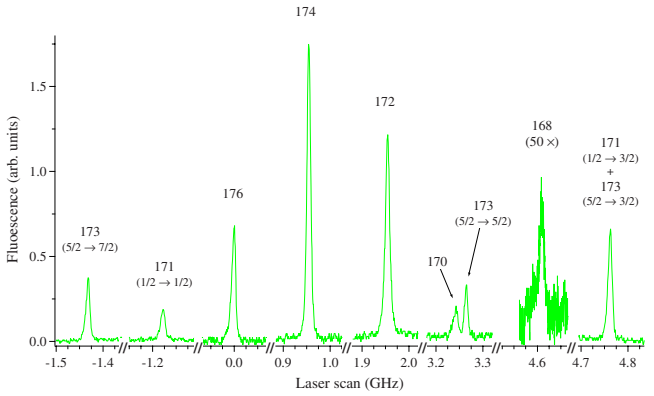

FIG. 2. (Color online) Yb spectrum showing fluorescence from the $^1S_0 \rightarrow {}^3P_1$ transition in the different isotopes. The scan is broken into nine smaller scans around each peak. The grid marks are 250 MHz apart and each narrow scan is 140 MHz wide. The gain of the photomultiplier tube (PMT) has to be increased by a factor of 50 to see the ^{168}Yb peak. The odd isotopes have hyperfine structure and are labeled as $F \rightarrow F'$. The last peak contains two overlapping transitions.

AOM2. Measurement of the frequency of AOM2 thus constitutes the frequency measurement. The two laser locks are achieved by modulation of the laser frequency and phase-sensitive demodulation using lock-in amplifiers. The cavity and the AOM2 are locked by modulating the cavity length (by dithering a piezomounted mirror) and demodulation using lock-in amplifiers. All the error signals used for locking are first harmonic except for the reference laser, where third-harmonic detection [12] is used to eliminate peak-pulling effects from any residual Doppler profile in the saturated-absorption signal.

A. Yb spectroscopy

Yb spectroscopy is done inside a vacuum chamber maintained at a pressure below 10^{-8} torr. The Yb atomic beam is produced by heating a quartz ampoule containing metallic Yb to a temperature of about 400 °C. Doppler broadening is minimized by having the laser beam intersect the atomic beam at right angles. Systematic Doppler shifts in frequency due to misalignment from perpendicularity are minimized by retroreflecting the laser beam. The resonance fluorescence from the atoms is imaged on to a photomultiplier tube (Hamamatsu, R928) through a narrow slit. The laser intensity is about 1 $\mathrm{mW/cm^2}$ compared to the saturation intensity of 0.14 $\mathrm{mW/cm^2}$.

A typical Yb spectrum is shown in Fig. 2. Since the source contains all isotopes in their natural abundances, the height of the peak for a particular isotope is proportional to its abundance. The rarest isotope ^{168}Yb has a natural abundance of only 0.14%, and hence the gain of the photomultiplier tube has to be increased by a factor of 50 to see this peak. For the odd isotopes which have hyperfine structure, the transition amplitude gets spread over the various hyperfine transitions. All the transitions are well resolved except for the last peak.

The line shape of the peaks is seen more clearly from the close-up of the ^{174}Yb transition shown in Fig. 3. The symmetry of the curve indicates that the retroreflected laser beam is close to being perpendicular. The solid curve is a fit to a Voigt profile to take into account residual Doppler broadening due to finite collimation of the atomic beam. This effect also causes the linewidth to be 6.2 MHz, compared to the natural linewidth of 180 kHz. The Voigt profile fits the data well, as seen from the featureless residuals. All the resolved transitions have the same line shape and width.

B. Separation of overlapping transitions

As mentioned above, the last peak in the spectrum consists of two overlapping transitions: $^{171}\mathrm{Yb}(1/2 \rightarrow 3/2)$ and $^{173}\mathrm{Yb}(5/2 \rightarrow 3/2)$. The linewidth of this combined peak is slightly larger than that of the resolved peaks. A two-peak fit with the linewidth fixed at the value for the ^{174}Yb spectrum and the relative amplitudes fixed at the expected ratio of 3.4 show that the separation between the two transitions is 2.9(4) MHz.

To resolve the two transitions, we have applied a longitudinal magnetic field. The different Landé g factors for the two isotopes imply that the sublevels shift by different amounts and are therefore separated. The field is produced by a pair of Helmholtz coils of 300 turns each with an average diameter of 60 mm and kept at a separation of 50 mm.

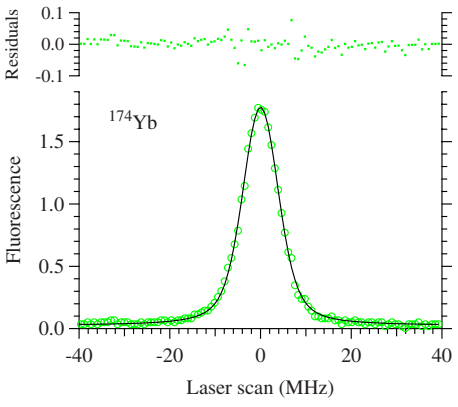

FIG. 3. (Color online) Close-up of the ^{174}Yb peak. The circles show the measured fluorescence signal. The solid line is a fit to a Voigt profile with the residuals shown on top.

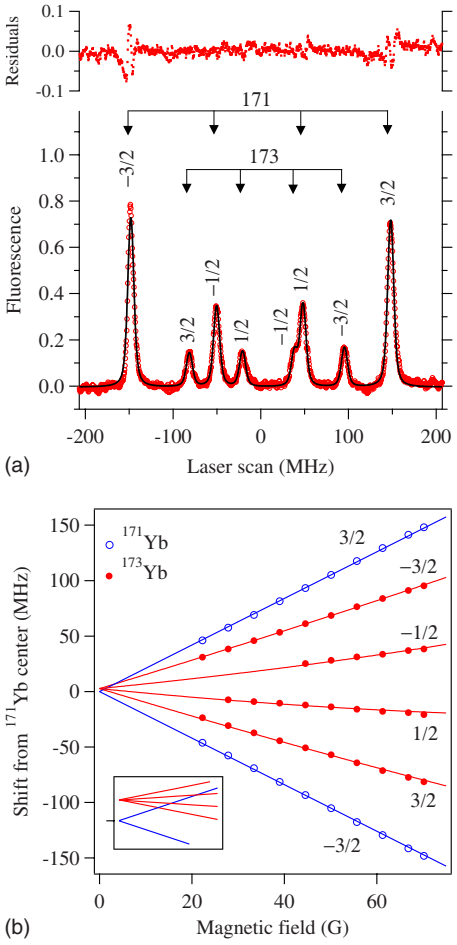

FIG. 4. (Color online) Separation of the ^{171}Yb$(1/2\rightarrow 3/2)$ and ^{173}Yb$(5/2\rightarrow 3/2)$ overlapping peaks using a magnetic field. In (a), we show a spectrum with a field of 70.2 G. The zero is at the location of the unshifted ^{171}Yb transition. The solid curve is a multipeak fit to extract the locations of the eight sublevels, with the fit residuals shown on top. In (b), we show the shift of the various sublevels in the two isotopes as a function of B field. The solid lines are fits to the calculated shifts, with the y intercept as the only fit parameter. The inset shows a close-up of the y intercept for the fits.

This guarantees that the field is uniform to better than a part in 3000 over the interaction region. Since it is difficult to measure the field accurately, we drive the coils with a precision current source. We study the shifts as a function of coil current and extrapolate to zero current and thus to zero field. The laser scan axis is calibrated by simultaneously exciting the atomic beam with an AOM-shifted laser beam that has a known frequency offset.

A typical spectrum with a current of 3.15 A (B =70.19 G) is shown in Fig. 4(a). The eight subtransitions (four in each isotope) are clearly identifiable. The goal is to find the offset between the zero-field points for two isotopes. To do this, we first calculate the shift in the subtransitions for each isotope as a function of the magnetic field B. Since the ground state is $^1S_0$, there is no appreciable shift of the ground sublevels, and one needs to consider only the shift of the excited-state sublevels. To account for off-diagonal coupling from the other hyperfine levels, we calculate the shift of the $|F,m_F\rangle$ sublevel using the full $|J,I,m_J,m_I\rangle$ basis, where $\mathbf{J}$ is the electronic angular momentum, $\mathbf{I}$ is the nuclear spin, and $\mathbf{F}=\mathbf{I}+\mathbf{J}$ is the total angular momentum. Let us first concentrate on the stretched sublevels, namely, $m_F=\pm 3/2$, which become resolved even at lower fields. For ^{171}Yb, we find that the shift is simply given by $\mu_B g_F m_F B$, where μ_B =1.4 MHz/G is the Bohr magneton and $g_F=1$ is the Landé g factor of the level. However, for ^{173}Yb, the $m_F=+3/2$ sublevel shifts by a larger amount compared to the $m_F=-3/2$ sublevel. The shifts are slightly different from that calculated using the Landé g factor of −0.6, but interestingly the separation between the two is still $2\mu_B g_F m_F B$, implying that the additional correction is exactly equal for the two sublevels.

To find the zero-field offset between the two transitions, we have to first determine precisely the current-to-field conversion factor. To do this, we plot the difference between the shifts of $m_F=\pm 3/2$ sublevels as a function of current. From our theoretical analysis, we know that this difference is just $3\mu_B g_F B$ for both isotopes. A linear fit yields the conversion factor as 22.28(3) G/A, which is consistent with the field of 22.37(10) G measured with 1 A of coil current.

With the current properly scaled to a magnetic field, the procedure for finding the zero-field offset proceeds as follows: (i) we first obtain the center of the ^{171}Yb transition, which is just the average of the $m_F=\pm 3/2$ sublevels since they shift by equal and opposite amounts; (ii) we then determine the shift of the $m_F=\pm 3/2$ sublevels in ^{173}Yb with respect to the above center; (iii) we plot the measured shift as a function of magnetic field; and (iv) we finally do a least-squares fit of the measured shift to the theoretically calculated one with the zero-field offset as the only fit parameter.

The shifts and the curve fits are shown in Fig. 4(b). We do *independent* fits to the two sublevels. The fit to the $m_F=+3/2$ sublevel gives an offset of 2.69(8) MHz, while the fit to the $m_F=-3/2$ sublevel gives an offset of 2.69(29) MHz. For comparison, the sublevels in ^{171}Yb vary with the same slope and the straight-line fits converge to an offset of zero, as expected. To gain further confidence in this value of offset, we have also analyzed the shifts of the $m_F=\pm 1/2$ sublevels in ^{173}Yb. As in the case of the stretched sublevels, the calculated shift is nonlinear and slightly different from the value calculated using the Landé g factor. A least-squares curve fit to the measured shifts of the $m_F=+1/2$ sublevel yields an offset of 2.68(25) MHz, consistent with the above values. For the $m_F=-1/2$ sublevel, the peak becomes separate from the $m_F=+1/2$ sublevel of ^{171}Yb only above a field of 45 G, so there are fewer points to fit. Still, the fit yields a consistent offset of 2.59(29) MHz. A combined fit to all the sublevels then gives an offset of 2.67(12) MHz.

As a further check on this separation, we have extracted the offset by using a two-peak fit to the combined spectrum. To determine the relative amplitudes, we sum the amplitudes of the sublevels in each isotope from the resolved spectra at the different magnetic fields. This gives the relative ratio as 3.37(10). If we now fix the two amplitudes to this ratio, and the line shape and width of each peak to that of the ^{174}Yb transition, we get a separation of 2.55(18) MHz. The combined spectrum with the two subpeaks is shown in Fig. 5. We have verified that the offset is around 2.6 MHz by fitting to 20 independent spectra, thus giving confidence in this value.

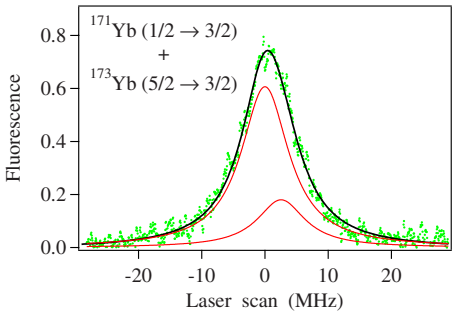

FIG. 5. (Color online) Two-peak fit to extract the offset between the overlapping ^{171}Yb$(1/2 \rightarrow 3/2)$ and ^{173}Yb$(5/2 \rightarrow 3/2)$ transitions.

The above analysis shows that the ^{173}Yb$(5/2 \rightarrow 3/2)$ transition is higher than the ^{171}Yb$(1/2 \rightarrow 3/2)$ one by 2.67(12) MHz. Since the frequency of the combined peak is measured by locking to the peak center, the two transition frequencies have to be obtained by adding corrections to the combined frequency. From the two-peak fit shown in Fig. 5, we determine that the first transition is 0.564(50) MHz to the left of the peak, and the second transition is 2.106(120) MHz to the right. The smaller uncertainty for the correction of the first peak is because this peak is quite prominent. Within the uncertainty of 50 kHz, the correction is insensitive to variations in linewidth of the two peaks, value of the offset, and up to $\pm 10\%$ variation in the amplitude of the second peak. Since we measure the amplitude ratio using the magnetically resolved spectra with an error of 3%, the error should account for this uncertainty. The above corrections are added to the measured frequency of the combined peak.

III. ERROR ANALYSIS

Our previous measurements using this technique [4,6–8], which have been absolute frequency measurements, have been measurements of optical transitions within 100 nm of the reference wavelength. In these cases, residual dispersion inside the cavity was not a significant problem. However, in the present case, the unknown wavelength is 225 nm away, and we found that even a few °C change in the room temperature caused the absolute frequency to vary. We verified this by studying the separation between a cavity mode and the ^{174}Yb transition. The cavity mode drifted around by a few MHz, and we could reduce this considerably by adding a thermal shield around the chamber. We also improved the vacuum inside the cavity, from 10^{-2} to 10^{-5} torr, and this improved the stability further. With the cavity locked to the reference laser, we then monitored the transition frequencies of ^{174}Yb and ^{176}Yb over a period of a few days. We found that the absolute frequency varied by about 5 MHz, but the difference remained the same to within 50 kHz.

A. Statistical errors

The primary sources of statistical error in our technique are fluctuations in the lock points of the lasers, and the cavity and the AOM2. To minimize such effects, we use an integration time of 10 s in the frequency counter used to measure the AOM frequency and then take an average of about 20 values for each measurement. This results in an overall statistical error of less than 10 kHz in a measurement.

B. Systematic errors in the difference frequency

Systematic errors can be classified under three categories: errors related to locking the reference laser, errors related to locking the unknown laser on the Yb line, and errors due to the measurement cavity.

Systematic errors related to the reference laser are important for absolute frequency measurements, but will cancel when taking the difference. Similarly, errors due to dispersion inside the cavity and at the cavity mirrors, as mentioned above, will not affect the difference. Potential errors due to geometric misalignment into the cavity are avoided by using a single-mode fiber to couple into the cavity. Thus, all the sources of systematic error in the difference frequency are related to how well we can lock the unknown laser to a particular Yb transition and how well we can lock the cavity to the laser.

Collisional shifts of the transition frequency are minimal because we use an atomic beam. There are three other potential sources of error:

(i) A systematic Doppler shift of the peak center could occur if the angle between the atomic beam and the laser beam is not exactly 90°. As mentioned earlier, this is minimized by using a retroreflected laser beam. Moreover, this will cause a systematic error in the difference frequency only to the extent that different isotopes come out of the oven with different velocities. The rms velocity varies from 307 m/s for ^{176}Yb to 314 m/s for ^{168}Yb, which means that the systematic error is 12.6 kHz for a misalignment of 1 mrad.

(ii) Systematic errors in peak position due to line-shape asymmetry that might occur because of selective driving into Zeeman sublevels (shifted in the presence of stray magnetic fields) or radiation pressure. The first effect is minimized by using linearly polarized light, so that the Zeeman sublevels are excited equally about line center. The size of this error is estimated by studying the asymmetry of the fluorescence line shapes (see Fig. 3).

(iii) Locking errors due to phase shifts in the different feedback loops. This error depends on the parameters of the loop such as gain and time constant. Our best handle on this error is to measure the same shift (say between ^{174}Yb and ^{176}Yb) using two different lock points of the reference laser, one from the $F=1 \rightarrow F'$ hyperfine manifold and the other from the $F=2 \rightarrow F'$ manifold. Changing the manifold implies a different set of cavity mode numbers, which in turn means reoptimizing all the feedback loops. There could be other sources of error related to higher-order cavity modes, which also contribute to the difference. Using a series of measurements with the two sets, we estimate these errors to be less than 50 kHz.

The estimated sizes of these errors are listed in Table I. The final error of 60 kHz is calculated by adding all these errors in quadrature with a statistical error of 10 kHz.

IV. RESULTS AND DISCUSSION

As mentioned in the previous section, a stringent check on our locking errors is to measure the shifts using different

TABLE I. Systematic errors in the difference frequency.

Source of error	Size (kHz)
(1) Misalignment from perpendicularity	13
(2) Peak shift due to line-shape asymmetry	30
(3) Locking errors and higher-order cavity modes	50

hyperfine transitions of the reference laser. Transitions starting from the $F=1$ and the $F=2$ ground levels differ by 6.5 GHz, and this ensures that we have the correct mode-number combination since the free-spectral range of the cavity is only 1.3 GHz. The results of these independent measurements are shown in Table II. The average value is consistent within the estimated error of 50 kHz. The measurements were repeated over a period of a few weeks to check against long-term drifts, particularly due to ambient temperature variations.

The average difference frequencies for the various isotopes are compared to previous work in Table III. The values are given as shifts from the transition frequency in ^{176}Yb and are quoted with an error of 60 kHz. As discussed earlier, the last two frequencies have to be obtained by adding corrections to the measured value of the overlapping peak. These two frequencies have slightly larger errors to account for errors in determining the corrections. Similarly, the transition in ^{168}Yb has much lower signal-to-noise ratio and is quoted with a larger error. The dispersion inside the cavity causes the absolute frequency to vary by a few MHz. Therefore, we are only able to determine the absolute frequency of the ^{176}Yb transition with a large error of 10 MHz as

$$539\ 385\ 606(10)\ \text{MHz}.$$

The results of previous measurements on this line are listed in columns 3–7 of Table III. The only work with sub-MHz precision is from Ref. [9]; all the others have errors ranging from 1 to 10 MHz. Our values are consistent with this precise earlier work at the 1σ level. This work was also the only measurement where the overlapping peak was resolved, using a magnetic field of 102 G. As shown earlier, our result for the difference between the two transitions is 2.67(12) MHz while the earlier value was 0.59(50) MHz. This is the only nonoverlapping result, but we have done several checks to gain confidence in our value.

TABLE II. Frequency shifts of various transitions in the 555.8-nm $^1S_0 \leftrightarrow {}^3P_1$ line in Yb. The first set is measured with the reference laser locked to a transition in the $F=1 \rightarrow F'$ manifold, while the second set is an independent measurement with the reference laser on the $F=2 \rightarrow F'$ manifold. The average value overlaps with the two measurements within our estimated error.

	Shift from ^{176}Yb (MHz)		
Transition	$F=1 \rightarrow F'$	$F=2 \rightarrow F'$	Average
$^{173}\text{Yb}(\frac{5}{2} \rightarrow \frac{7}{2})$	−1431.892	−1431.851	−1431.872
$^{171}\text{Yb}(\frac{1}{2} \rightarrow \frac{1}{2})$	−1177.261	−1177.201	−1177.231
^{176}Yb	0	0	0
^{174}Yb	954.800	954.863	954.832
^{172}Yb	1954.828	1954.876	1954.852
^{170}Yb	3241.169	3241.184	3241.177
$^{173}\text{Yb}(\frac{5}{2} \rightarrow \frac{5}{2})$	3266.219	3266.267	3266.243
^{168}Yb	4609.888	4610.031	4609.960
$^{171}\text{Yb}(\frac{1}{2} \rightarrow \frac{3}{2}) + {}^{173}\text{Yb}(\frac{5}{2} \rightarrow \frac{3}{2})$	4759.979	4760.029	4760.004

Hyperfine structure in ^{171}Yb and ^{173}Yb

We have used the data in Table III to obtain the hyperfine-coupling constants in the $6s6p\ ^3P_1$ state of the odd isotopes ^{171}Yb and ^{173}Yb. For ^{171}Yb, there are two hyperfine levels, and their transition frequencies are used to calculate the magnetic dipole coupling constant A and the position of the centroid. For ^{173}Yb, there are three hyperfine levels in the excited state. The three transition frequencies are used to calculate the magnetic dipole coupling constant A, the electric quadrupole coupling constant B, and the position of the centroid.

TABLE III. Frequency shifts of various transitions compared to previous work on this line.

	Shift from ^{176}Yb (MHz)					
Transition	This work	Ref. [9]	Ref. [13]	Ref. [14]	Ref. [15]	Ref. [16]
$^{173}\text{Yb}(\frac{5}{2} \rightarrow \frac{7}{2})$	−1431.872(60)	−1431.73(50)	−1432.6(12)	−1432.5(43)	−1460(6)	−1451(6)
$^{171}\text{Yb}(\frac{1}{2} \rightarrow \frac{1}{2})$	−1177.231(60)	−1177.23(50)	−1177.3(11)	−1176.6(35)	−1187(3)	−1184(6)
^{176}Yb	0	0	0	0	0	0
^{174}Yb	954.832(60)	954.76(50)	954.2(9)	953.0(13)	947(2)	947(2)
^{172}Yb	1954.852(60)	1955.04(50)	1954.8(16)	1954.0(26)	1940(9)	1940(9)
^{170}Yb	3241.177(60)	3241.51(50)	3241.5(28)	3239.6(40)	3229(18)	3232(6)
$^{173}\text{Yb}(\frac{5}{2} \rightarrow \frac{5}{2})$	3266.243(60)	3266.49(50)	3267.1(28)	3264.3(98)	3247(9)	3253(6)
^{168}Yb	4609.960(80)	4610.14(50)	4611.9(44)	4609.5(54)	4581(15)	
$^{171}\text{Yb}(\frac{1}{2} \rightarrow \frac{3}{2})$	4759.440(80)	4759.83(50)	4761.8(37)	4759.5(143)	4761(9)	4761(9)
$^{173}\text{Yb}(\frac{5}{2} \rightarrow \frac{3}{2})$	4762.110(120)	4760.42(50)	4761.8(37)	4759.5(143)	4749(12)	4700(6)

TABLE IV. Center of gravity (c.g.) and hyperfine constants in the odd isotopes. All units are in MHz.

Isotope		This work	Ref. [9]
^{171}Yb	c.g. from ^{176}Yb	2780.550(56)	2780.81(50)
	A	3957.781(63)	3957.97(47)
^{173}Yb	c.g. from ^{176}Yb	1510.607(39)	1510.38(50)
	A	−1094.328(19)	−1094.20(60)
	B	−826.635(67)	−827.15(47)

The calculated hyperfine constants and centroid locations are compared to previous values from Ref. [9] in Table IV. Despite the significant difference between the values for the offset of the overlapping transition, the two sets of hyperfine constants are consistent at the 1σ level.

V. CONCLUSIONS

In conclusion, we have measured the frequencies of various components in the 555.8-nm $^1S_0 \rightarrow {}^3P_1$ intercombination line in Yb. The frequencies are measured using an evacuated ring-cavity resonator stabilized to the D_2 line of Rb. The Yb line is accessed with a frequency-doubled fiber laser. We obtain a precision of 60 kHz in the measurement of the difference frequencies used in calculating isotope shifts and hyperfine structure. This represents an order-of-magnitude improvement over the previous work. This work should complement our earlier work on the 399-nm $^1S_0 \rightarrow {}^1P_1$ line in Yb [8]. Accurate knowledge of isotope shifts and hyperfine constants in the $^1P_1$ and the $^3P_1$ states will help in fine tuning atomic wave functions used in theoretical calculations, which are important in interpreting ongoing experiments in parity and time-reversal symmetry violations.

ACKNOWLEDGMENTS

We thank Challenger Mishra for help with the Zeeman shift calculations and Vaideesh Loganathan for help with the data analysis. This work was supported by the Department of Science and Technology and the Board of Research in Nuclear Sciences (DAE), Government of India. One of us (K.P.) acknowledges financial support from the Council of Scientific and Industrial Research, India.

[1] J. E. Stalnaker, D. Budker, S. J. Freedman, J. S. Guzman, S. M. Rochester, and V. V. Yashchuk, Phys. Rev. A **73**, 043416 (2006).
[2] V. Natarajan, Eur. Phys. J. D **32**, 33 (2005).
[3] A. Dilip, B. P. Das, and F. Warren, J. Phys. B **34**, 3089 (2001).
[4] A. Banerjee, D. Das, and V. Natarajan, Opt. Lett. **28**, 1579 (2003).
[5] A. Banerjee, U. D. Rapol, and D. Das, EPL **63**, 340 (2003).
[6] D. Das, A. Banerjee, S. Barthwal, and V. Natarajan, Eur. Phys. J. D **38**, 545 (2006).
[7] Dipankar Das and Vasant Natarajan, Phys. Rev. A **75**, 052508 (2007).
[8] D. Das, S. Barthwal, A. Banerjee, and V. Natarajan, Phys. Rev. A **72**, 032506 (2005).
[9] D. L. Clark, M. E. Cage, D. A. Lewis, and G. W. Greenlees, Phys. Rev. A **20**, 239 (1979).
[10] J. Ye, S. Swartz, P. Jungner, and J. L. Hall, Opt. Lett. **21**, 1280 (1996).
[11] A. Banerjee, U. D. Rapol, A. Wasan, and V. Natarajan, Appl. Phys. Lett. **79**, 2139 (2001).
[12] A. J. Wallard, J. Phys. E **5**, 926 (1972).
[13] W. A. van Wijngaarden and J. Li, J. Opt. Soc. Am. B **11**, 2163 (1994).
[14] W. G. Jin, T. Horiguchi, M. Wakasugi, T. Hasegawa, and W. Yang, J. Phys. Soc. Jpn. **60**, 2896 (1991).
[15] G. E. Millerand and J. Ross, J. Opt. Soc. Am. **66**, 585 (1976).
[16] Y. Chaiko, Opt. Spectrosc. **20**, 424 (1966).